

Morphology of perineal lacerations and episiotomy

Zbyněk Tonar^{1,2}, Vladimír Kališ³, Petra Kochová¹

¹Department of Mechanics, Faculty of Applied Sciences, University of West Bohemia in Pilsen

²Department of Histology and Embryology, Charles University, Faculty of Medicine in Pilsen

³Department of Obstetrics and Gynaecology, University Hospital in Pilsen, Czech Republic

zbynek.tonar@lfp.cuni.cz

zcu.jpg

logofav_en.jpg

lfpznak1.png

Introduction

Evidence-based medicine does not support all the maternal benefits traditionally ascribed to routine episiotomy. The range of obstetric perineal injury was suggested to be influenced by concurrent vaginal infection and inflammation of the wall of vagina.

Microstructure of the vagina

The vagina has an inner mucosal and an external muscular layer. The lamina propria of the mucosa contains many thin-walled veins below the stratified squamous epithelium. The muscular layers are composed of smooth muscle and consists of a thick outer longitudinal and an inner circular layer. Longitudinal fibres are continuous with the superficial muscle fibres of the uterus, and the strongest fasciculi are those attached to the rectovesical fascia on each side. The two layers are not distinct but connected by oblique decussating fasciculi. The lower vagina is also surrounded by the skeletal muscle fibres of bulbospongiosus. A layer of loose connective tissue, containing extensive vascular plexuses, surrounds the muscle layers.

Aims

The aim of this pilot study was to design a histological protocol for quantitative assessment of rupture proneness of perineum at the time of vaginal birth.

Material and methods

In this pilot study, we analyzed one sample of the wall of vagina ($10 \times 5 \times 5$ mm), taken away from the edge of a rupture which had occurred during the labour, and two control samples taken away from the edge of routine episiotomy. All patients gave their informed consent. We performed a multistage systematic random sampling at the level of tissue block and at the level of serial sections. We used hematoxylin-eosin and green trichrome stains to examine the overall morphology of the sample and immunohistochemistry in order to detect CD68+ cells infiltrating the vagina wall as well as smooth muscle cells containing the α -SM actin.

Quantification

In the sections under study, we assessed the **area of haemorrhages** according to the Equation 1:

$$estA = a \cdot P \quad (1)$$

where $estA$ is the estimated area, grid parameter a is the area corresponding to one test point and P is the number of test points hitting the haemorrhages. Cavalieri principle was used for estimation of the volume V of the haemorrhages within the total reference volume of the tissue sample, see Equation 2:

$$estV = T \cdot (A_1 + A_2 + \dots + A_m) \quad (2)$$

where $estV$ is the Cavalieri volume estimator, $T = 0.030$ μm is the distance between two following selected sections, and A_i is the area of lesion in the i -th section. We evaluated eight sections as representatives of each tissue sample, i.e. ($m = 8$). This gave us a ratio (Equation 3):

$$haem(ratio) = \frac{estV(haem)}{estV(total)}, \quad (3)$$

where $haem(ratio)$ is the relative proportion of the haemorrhages $estV(haem)$ within the tissue $estV(total)$. As the covering vaginal epithelium was free of blood vessels, its volume was not considered to be a part of the $estV(total)$. Disector principle was used for **estimation of numerical density** $estN_V(par)$ of CD68+ cells in the within the reference sample brick, see the Equation 4.

$$estN_V(par) = \frac{\sum_{i=1}^n Q_i^-(par)}{\sum_{i=1}^n P_i(ref)} \cdot \frac{p}{a \cdot h}, \quad (4)$$

where $estN_V(par)$ is the estimated number of particles within the reference volume, n is the number of disectors (sampling bricks), $Q_i^-(par)$ is the number of particles (cells) sampled by the i -th disector, $P_i(ref)$ is the number of points of the p -point grid in the i -th frame hitting the reference space, a is the actual area of the frame, and h denotes the height of the disector. We used two methods:

physical disector – two physical sections (thickness of 5 μm) were used so that they had been to be registered with respect to the Z -axis,

optical disector – four sections (thickness of 5 μm) were created optically by a $100\times/1.25$ oil immersion objective within a 20 μm thick slices and the counting frame rules [2] were applied.

For each of the types, five disector sample volumes were applied to the samples under study. To perform the point-counting as well as the disector method, we used the software Ellipse3D (ViDiTo, Košice, Slovakia).

Coefficient of error (CE)

To assess the sampling error, we used the Gundersen and Jensen's method to predict the CE of the Cavalieri estimate [1], see Equations 5 and 6:

$$estCE_n = \frac{1}{\sum_{i=1}^n a_i} \cdot \sqrt{\frac{3A + C - 4B}{12}}, \quad (5)$$

$$A = \sum_{i=1}^n a_i \cdot a_i, \quad B = \sum_{i=1}^{n-1} a_i \cdot a_{i+1}, \quad C = \sum_{i=1}^{n-2} a_i \cdot a_{i+2}. \quad (6)$$

Results and discussion

Two parameters were suggested to be suitable for quantitative assessment of inflammatory reaction:

volume of haemorrhage was estimated with use of Cavalieri principle (Fig. 1–4, 7–10),

numerical density of CD68-positive cells (i.e. monocytes, macrophages, neutrophils, and large lymphocytes) was estimated by physical and optical disector (Fig. 11–14, Table 1).

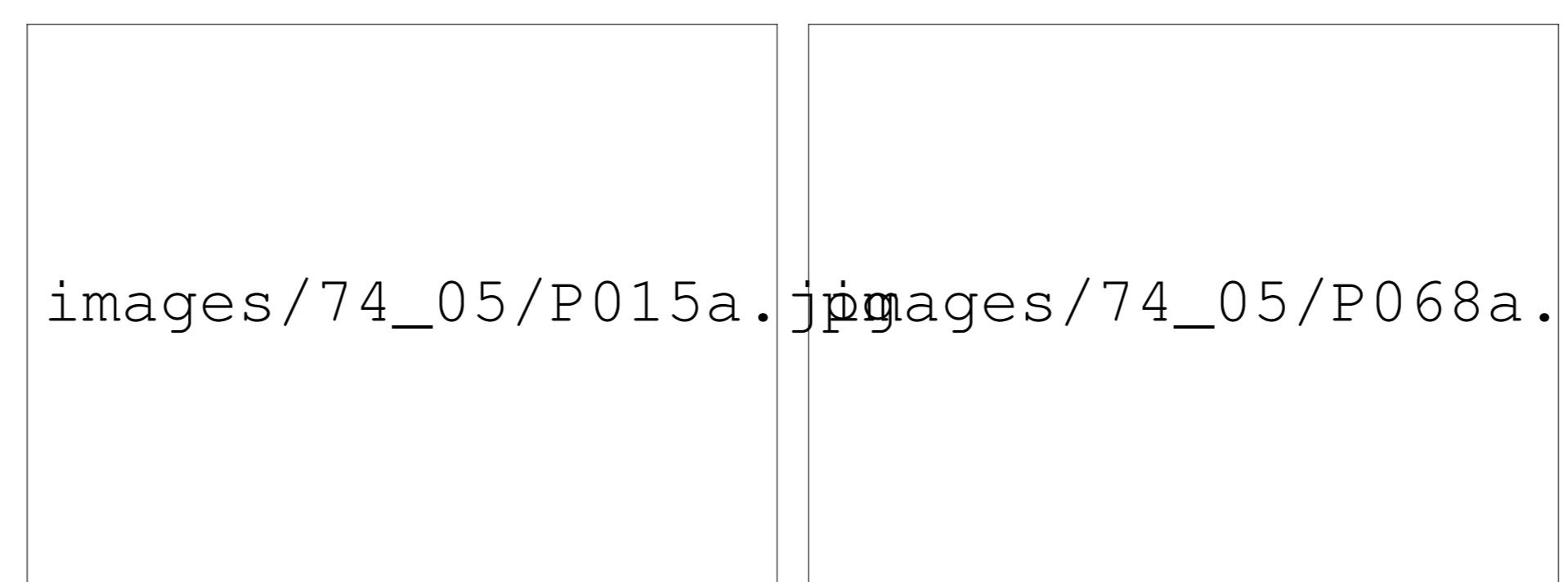


Fig. 1: Vaginal epithelium, subepithelial connective tissue with haemorrhage. Rupture sample with $haem(ratio) = 0.3767$.



Fig. 2: Dttto, green trichrome stain with Verhoeff's haematoxylin.

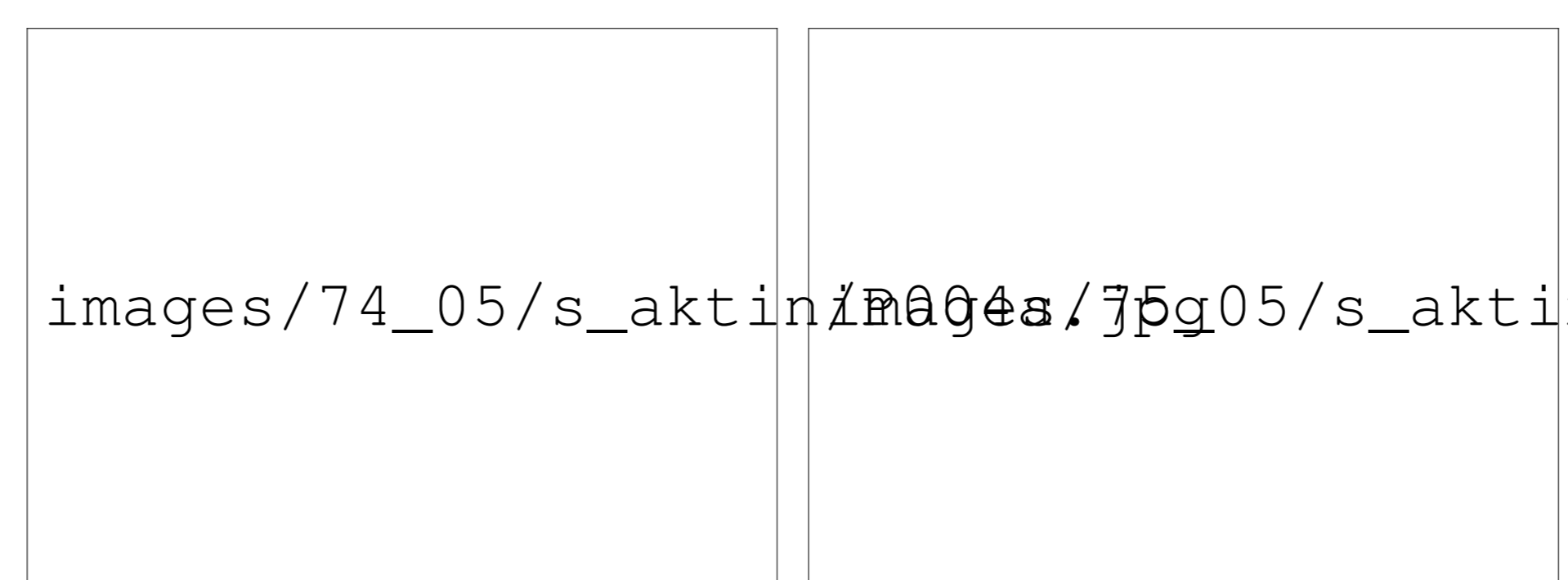


Fig. 3: Vaginal epithelium, subepithelial connective tissue with capillaries and haemorrhage. Rupture sample.

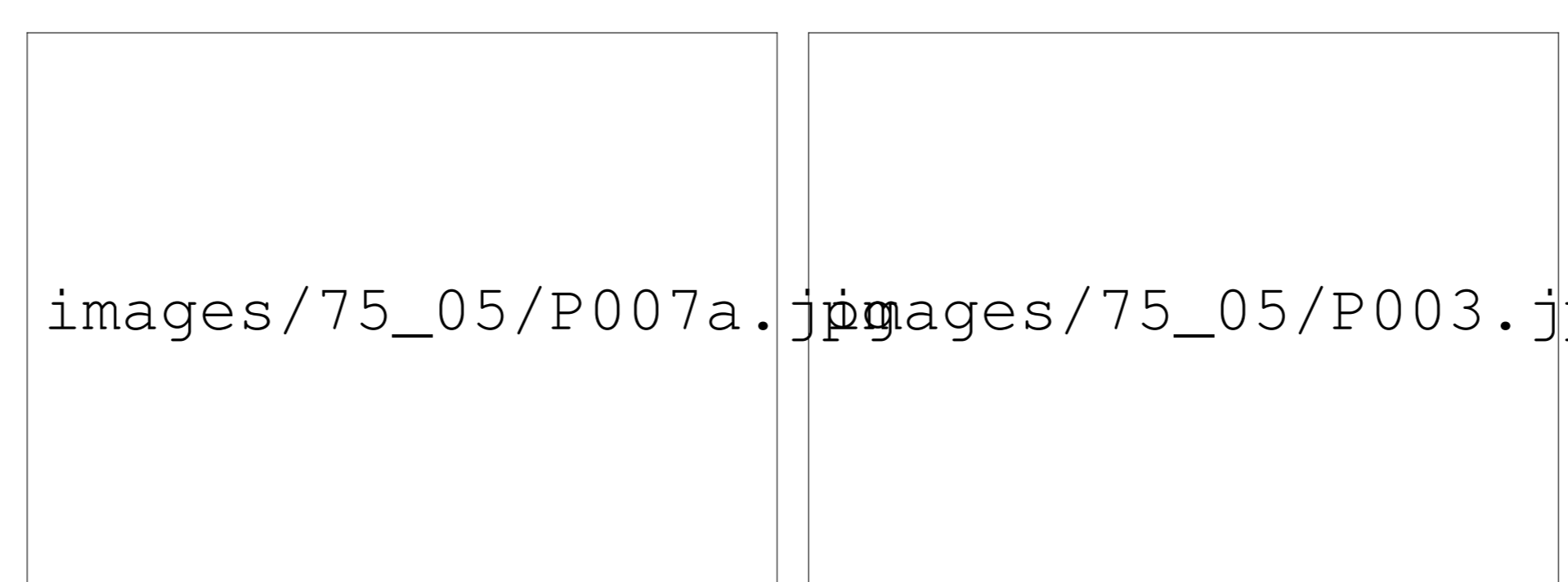


Fig. 4: Deeper layer of the wall of vagina.



Fig. 5: Smooth muscle cells in the walls of blood vessels within the subepithelial connective tissue. Control sample.

The analysis of CE of Cavalieri sections proved that it was appropriate to sample 8 sections within the total number of 48 sections.



Fig. 9: CE analysis, control sample.

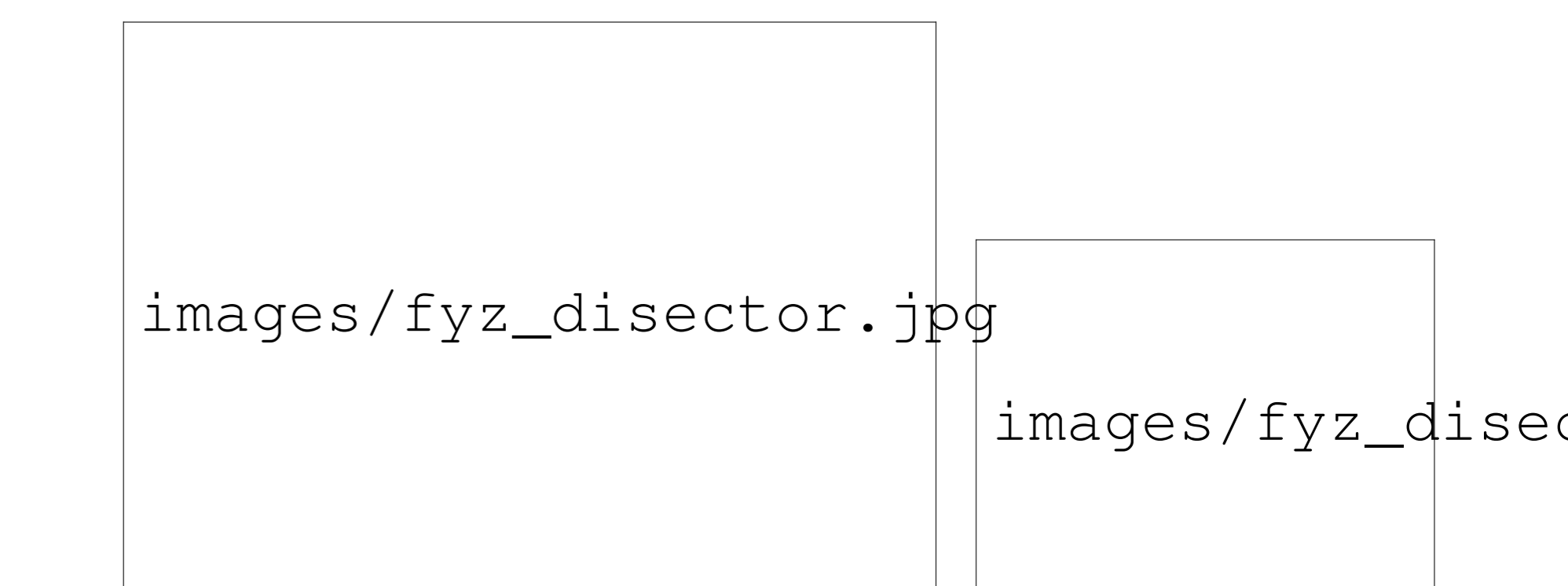


Fig. 10: Analysis of the sampling procedure.



Fig. 11: Physical disector (accepted cells marked as green, rejected cells are red), $estN_V(par) = 62508.92435$ cells/mm⁻³.

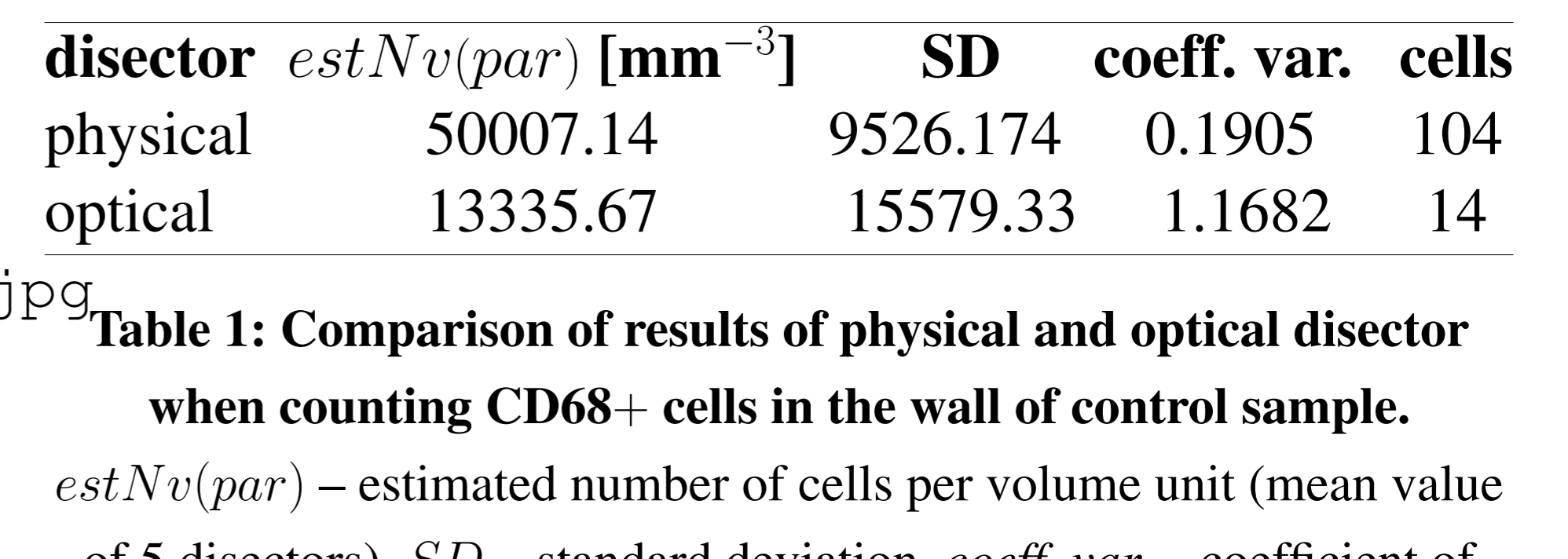


Fig. 12: A 3-D view of the same physical disector, control sample.

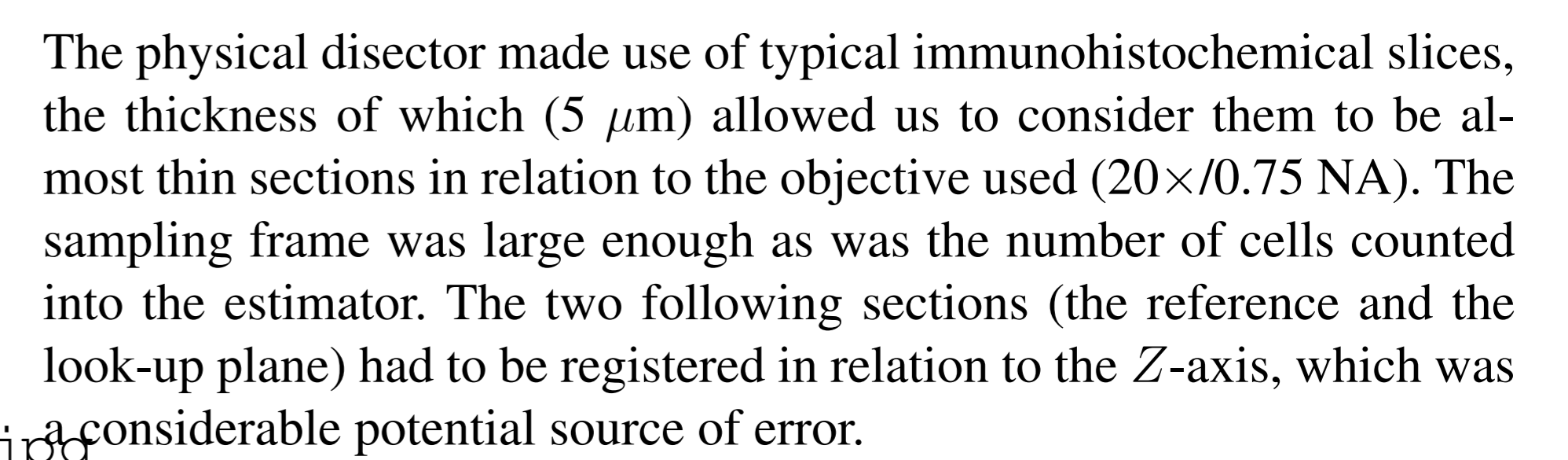


Fig. 13: Optical disector (accepted cells marked as green, rejected cell is red), $estN_V(par) = 14288.21946$ cells/mm⁻³.

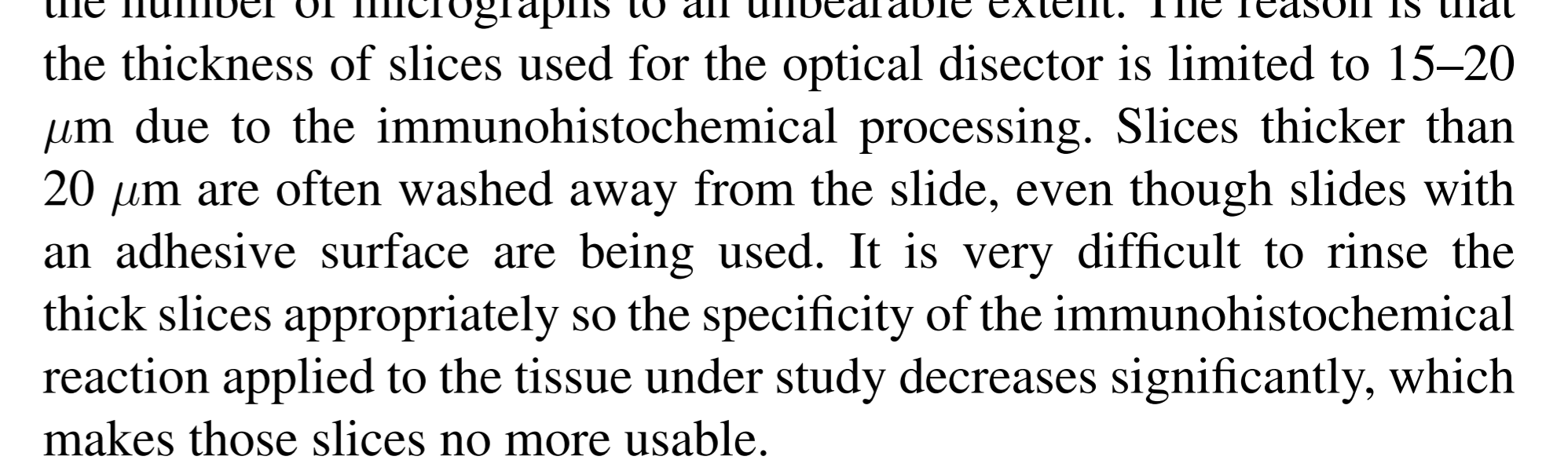


Fig. 14: A 3-D view of the same optical disector, control sample.

disector $estN_V(par)$ [mm⁻³] **SD** **coeff. var.** **cells**
 physical 50007.14 9526.174 0.1905 104
 optical 13335.67 15579.33 1.1682 14

Table 1: Comparison of results of physical and optical disector when counting CD68+ cells in the wall of control sample.
 $estN_V(par)$ – estimated number of cells per volume unit (mean value of 5 disectors), SD – standard deviation, $coeff. var.$ – coefficient of variation, $cells$ – total number of cells counted in 5 disectors.

The physical disector made use of typical immunohistochemical slices, the thickness of which (5 μm) allowed us to consider them to be almost thin sections in relation to the objective used ($20\times/0.75$ NA). The sampling frame was large enough as was the number of cells counted into the estimator. The two following sections (the reference and the look-up plane) had to be registered in relation to the Z -axis, which was a considerable potential source of error.

In order to achieve a higher total number of cells counted in the optical disector, a much more extensive sampling would be required. This would have surely reduced the sampling variability, but it would have increased the number of micrographs to an unbearable extent. The reason is that the thickness of slices used for the optical disector is limited to 15–20 μm due to the immunohistochemical processing. Slices thicker than 20 μm are often washed away from the slide, even though slides with an adhesive surface are being used. It is very difficult to rinse the thick slices appropriately so the specificity of the immunohistochemical reaction applied to the tissue under study decreases significantly, which makes those slices no more usable.

Conclusions of the pilot study

1. For further estimating the numerical density of cells in the wall of vagina, the physical disector will be used instead of the optical, since the results of physical disector had a lower variability.
2. The sampling strategy used for Cavalieri method of estimation of relative volume proportions of haemorrhage within the wall of vagina was based on systematic uniform random sampling, the variability of which was low enough.

Acknowledgement:
 This work was supported by the grant GAČR 106/04/0201.

References
 [1] Gundersen H.J.G., Jensen E.B. (1987): The efficiency of systematic sampling in stereology and its prediction. *J. Microsc.* 147:229–263.
 [2] Kubinova L., Janacek J.: Confocal microscopy and stereology: estimating volume, number, surface area and length by virtual test probes applied to three-dimensional images. *Microsc. Res. Tech.* 2001, 53:425–35.
 [3] Tomori Z., Kerkule I., Kubinova L. (2001): Disector program for unbiased estimation of particle number, numerical density and mean volume. *Image Anal. Stereol.* 20:119–130.